A displacement-detection based approach for process monitoring and processing window definition of resistance welding of thermoplastic composites

H. Shi, I. Fernandez Villegas*, H.E.N. Bersee

Structural Integrity & Composite, Faculty of Aerospace Engineering, Delft University of Technology, Kluyverweg 1, 2629HS, Delft, The Netherlands

* Corresponding author: Irene Fernandez Villegas (I.FernandezVillegas@tudelft.nl)

Tel: +31(0)15 278 9745; Fax: +31(0)15 278 1151

Email of other authors: H.Shi@tudelft.nl (H. Shi); H.E.N.Bersee@tudelft.nl (H.E.N. Bersee)

Abstract

The evolution of weld displacement, or the thickness of welding stack, with welding time during resistance welding of thermoplastic composites was characterized, and based on this the possibility of using displacement data for process monitoring and processing window definition was investigated. Resistance welding of glass fabric reinforced polyetherimide using a metal mesh as the heating element was studied, and weld displacement was detected using a laser sensor. The effect of welding parameters on the displacement curve was studied. Welding defects, such as voids and squeeze flow, could be detected by monitoring the weld displacement. Fast definition of the welding processing window was found to be possible using displacement curves, and

the predicted processing window showed good agreement with the processing window determined from mechanical tests.

Keywords

A. Polymer-matrix composites (PMCs); A. Thermoplastic resin; E. Joints/joining

1. Introduction

Resistance welding, a technology to join two materials using resistive heating of a heating element placed at the interface, is a time and cost-effective joining method for thermoplastic composites [1-3]. The resistance welding process needs to be well controlled to get good welding quality, in particular for applications in the aircraft industry. The main process parameters in resistance welding are input power, heating time and welding pressure. The welding pressure, which needs to be applied throughout the welding process, promotes intimate contact between the welding surfaces and prevents de-consolidation of the adherends. The input power determines how fast the welding temperature can be reached at the welding interface and hence how steep the through-the-thickness temperature gradient is. For each input power level there is a range of heating times that lead to welded joints with a sufficient degree of consolidation in absence of thermal degradation [3,4]. Within the development of resistance-welded thermoplastic composite structures, processing windows, which establish the combinations of input power and heating time that provide acceptable welds for a certain welding pressure, must be defined.

Processing windows for resistance welding are usually defined through mechanical testing, e.g. measuring the strength of the joints welded over a series of heating times for different power levels and comparing the strength values so obtained with a

threshold value [5-10]. The heating time that results in a higher weld strength than the threshold for each power level is regarded to be within the processing window. This method requires, however, a large number of tests, which are time consuming and costly. Research on process modelling of resistance welding of thermoplastic composites [11-16] has made it possible to define processing windows based on welding temperature and consolidation degree as simulated through a process model [14,16,17]. The accuracy of this method, deeply related to the quality of the data entered in the model, has nevertheless not yet been fully validated. In literature [14,16], the predicted processing windows have sometimes been found to be slightly larger than the processing window defined using mechanical tests, especially for welding at a low power input.

An alternative approach entails the definition of the right heating time through in-situ process monitoring in closed-loop resistance welding processes. Villegas proposes in [18] a method for process control of resistance welding based on indirect temperature feedback from monitoring the resistance of the heating element. Despite the straightforwardness of this method, different ways of characterizing the resistance versus temperature relationship of the heating element can lead to significant temperature deviations. Additionally, the resistance data cannot be directly linked to the quality of the welded joints. For this purpose, a relationship between welding temperature and joint quality has to be defined, for instance via mechanical testing. Since the reduction of the weld line thickness and the lap shear strength of welded joints are related [5,7,19], monitoring the weld line thickness during welding could be another possible way for the definition of processing windows as well as for process monitoring. The thickness of the weld line is however difficult to measure during the welding

process, but the vertical displacement of the whole welding stack (i.e. adherends and heating element), known as "weld displacement curve" or "melting curve" [7], can be more easily monitored [5,7]. During resistance welding the thickness of the welding stack is influenced by thermal expansion/contraction, weld consolidation/deconsolidation and resin squeeze flow. Extending the basic Duhamel-Newman relation [20], the strain of the welding stack, ε, can be expressed by:

$$\varepsilon = S\Delta\sigma + \alpha\Delta T \pm \beta\Delta X - \Delta\varepsilon_{consolidation} + \Delta\varepsilon_{deconsolidation} - \Delta\varepsilon_{flow}, \qquad (1)$$

where σ is stress, T is temperature, X is the crystallinity of matrix (applicable to semi-crystalline polymers), S is the material compliance, α is thermal expansion, β is crystallization induced volume shrinkage, $\varepsilon_{consolidation}$ is consolidation-induced strain, mainly due to intimate contact, $\varepsilon_{deconsoliadtion}$ is deconsolidation-induced strain, including void generation, and ε_{flow} is strain related to thickness reduction caused by resin squeeze flow. Thermal expansion and contraction have been identified in the weld displacement curves [7]. Nevertheless, a deeper understanding of such curves and their relationship with the weld quality is still needed, especially for state-of-the-art resistance welding with a metal mesh heating element [5,21,22].

In this study, resistance welding displacement curves were analysed, and the possibilities of using displacement data for process monitoring and processing window definition were explored. Firstly, the relations between the physical phenomena occurring during the welding process and the weld displacement curve were investigated. Secondly, the influence of welding parameters, such as power input, time and welding pressure, as well as the quality of the composite adherends on the weld displacement curve was studied. Thirdly, a method was proposed to define adequate

ranges of heating times for different power levels based on the weld displacement curve and validated through mechanical testing.

2. Experimental

2.1. Material and heating element

The material used for the welding experiments was made of 8 layers of 8HS satin woven glass fabric reinforced polyetherimide (GF/PEI), CETEX® from TenCate, The Netherlands, with a stacking sequence of $[(0/90)]_{4S}$. The GF/PEI laminates, with dimensions 580 mm × 580 mm, were consolidated in a hot platen press at a processing temperature of 320 °C and under a consolidation pressure of 2.0 MPa for 20 min. The resulting 1.8 mm-thick laminates were inspected using ultrasonic C-scan and cut into 192 mm × 100 mm adherends using a water-cooled diamond saw.

A plain woven stainless steel (AISI 304L) mesh with wire diameter of 0.04 mm and open gap of 0.09 mm was used as the heating element. Mesh strips of 250 mm × 13 mm were cut from a big sheet of mesh and used for the welding process. To provide a resin rich area at the welding interface, the meshes were impregnated with two layers of 60 µm thick PEI resin films in a hot platen press at a processing temperature of 300 °C and under a consolidation pressure of 0.3 MPa for 2 min, prior to the welding process. The impregnated meshes had a final thickness of approximately 0.08 mm.

2.2. Resistance welding

An in-house developed setup was used [23] for resistance welding of the adherends. A computer controlled power supply unit, Delta Elektronika, with a maximum DC output of 45 A and 70 V, was used to provide the welding energy. Two pneumatic systems were used to apply the welding pressure and clamping pressure individually. Two blocks of high-density fibre (HDF) wood were used as insulators placed below and

above the welding assembly, and the welding pressure was applied on the top insulator. Two GF/PEI adherends were single-lap welded with an overlap length of around 15 mm, with 1 mm-wide gap left on both sides of the mesh at the welding overlap, as shown schematically in Fig.1. The welding process was in all cases performed under a constant power input and a constant welding pressure

During welding, vertical displacement was measured using a laser sensor, LK-G series from KEYENCE, U.S., with ± 0.5 µm system error, which was vertically pointed to the top surface of the top insulator holder. The welding and displacement measurement setups are shown in Fig.2. Three weld displacement curves were obtained for each set of welding conditions used in this research in order to check the repeatability of the measurements. Average weld displacement curves are shown in the Results section of this paper. It must be noted that the displacement reading provided by the laser sensor was a combination of thickness changes in the welding stack and in the insulation blocks during welding. The displacement of the welding stack alone could not be directly measured due to the fact that it was covered by the insulation blocks during the whole welding process. As shown and explained in the Results section of this paper, this approach consisting of measuring the combined displacement of the welding stack and the insulation blocks, was still able to provide sufficient insight into the physical transformations caused by the welding process in the welding stack, i.e. adherends and heating element.. The resistance welding process was controlled by a Labview program, and all the parameters, such as current, voltage, temperature and displacement, were recorded during the welding process using a data acquisition system.

2.3. Testing methods

Single lap shear tests were performed on the resistance welded joints according to the ASTM D1002 standard to evaluate the welding quality. Six specimens with a width of 25.4 mm were cut from each welded assembly, and they were tested using a Zwick/Roell 250 KN testing machine with a constant crosshead speed of 1.3 mm/min. The tests were performed at room temperature (20 ± 3 °C) with a relative humidity of 50 ± 5 %. The apparent lap shear strength (LSS) of each specimen was calculated by dividing the maximum load by the overlap area of the joints, where the overlap area was calculated using the width of the specimen and the width of the heating element (13 mm). The results for all six specimens were used to calculate an average lap shear strength and corresponding standard deviation for the corresponding set of welding conditions used to produce each welded assembly. Cross-sections of the welded specimens were examined using optical microscopy.

In some of the experiments performed, the welding temperature was measured at the welding interface using 0.1 mm-diameter K-type thermocouples. The head of the thermocouples was insulated with Kapton ®, polyimide tapes, DuPont™, to prevent any electrical contact during welding. Owing to the non-uniform temperature distribution along and across the weld line, which is a well-known phenomenon in resistance welded joints [16], care was taken to always place the thermocouples at the same location. This location was midway between the electrical connectors, i.e. middle of the weld in the longitudinal direction, and at the middle of the overlap in the transverse direction (see Figure 1). With regards to the through-the-thickness direction, the thermocouple was placed between the impregnated mesh and the uppermost adherend. Temperature

measurements were performed on extra samples to prevent any possible influence of the thermocouples on the displacement measurement and on the LSS values.

GF/PEI laminates can absorb moisture from the surroundings after manufacturing and this residual moisture might result in void formation during the welding process [24,25]. As a result, moisture content in the adherends was measured by weighing them before and after drying in at oven at 135 °C. Laminates with 0.1wt.% moisture (stored in the lab for one week after manufacturing) were mostly used in this research to prove the suitability of using the weld displacement curves for process monitoring and process window definition even in the potential event of void formation.

3. Results and discussion

3.1. Analysis of the weld displacement curve

GF/PEI laminates with 0.1 wt% residual moisture were resistance welded using a constant power input of 80 kW/m^2 under a constant welding pressure of 0.8 MPa and 100 s heating time. The evolution of welding temperature and average weld displacement with time are shown in Fig.3. It must be noted that for this and all the different experiments presented in what follows the three weld displacement curves used to calculate the presented average displacement showed a high degree of repeatability. The following five stages could be identified in the displacement curve:

Stage i, which happens at the beginning of the welding process and is characterised by the absence of significant displacement. It is believed to be influenced by the action of two opposing phenomena, overall thermal expansion and intimate contact at the welding interface. Even though pre-consolidated laminates and impregnated heating elements were used for resistance welding, some gaps can be expected to still exist at the contact

interfaces, resulting from micro-asperities on the surfaces. As a result, a decrease in thickness of the welding stack can be expected until intimate contact is achieved. It must be noted that the end of stage i coincides approximately with the moment when the glass transition temperature of PEI (T_g = 215°C) was reached at the welding interface. At that point, the PEI resin is expected to be soft enough to allow for full intimate contact through surface deformation.

Stage ii, characterised by a fast rising displacement until a peak is reached. Two of the causes for the thickness increase measured in stage ii are thermal expansion of the welding stack, potentially amplified by an increase in the coefficient of thermal expansion of PEI above its glass transition temperature [26] as well as thermal expansion of the insulators. Another phenomenon contributing to the thickness increase is void generation in the adherends, shown in Fig. 4 and believed to be caused by residual moisture and/or de-compaction during the welding process [7,19,22],

Stage iii, characterised by a clear drop in the displacement curve which is attributed to the occurrence of squeeze flow at the welding interface. Even though thermal expansion and void formation will still cause positive displacement, the negative displacement induced by resin squeeze flow is certainly dominant in this stage.

Stage iv, which onset coincides with the moment in which the power supply was switched off and is characterised by a continuous drop in the displacement curve. Volumetric contraction is believed to be the dominant physical phenomena in this stage. Nevertheless, heat conduction from the weld interface to the surrounding materials could still cause thermal expansion far from the weld interface and thus provide a positive component to the total displacement. After the temperature of the weld drops below the T_g of PEI, displacement decreases at a lower rate.

Stage v, in which no significant displacement can be observed anymore. In this stage, the contraction of the joint should be roughly equal to the thermal expansion of the areas far from the weld interface. As shown in Fig.5, the temperature in the insulation blocks continues to increase long after the power has been switched off. Eventually, all thermal expansion/contraction will cease when the temperature becomes stable. It is interesting to note that a final positive displacement was obtained, indicating that the final thickness of the measured stack was higher than its initial thickness. This thickness increment is believed to result from the porosity induced by the welding process in the adherends (Fig. 4).

3.2. Effect of heating time on the weld displacement curve

Fig. 6 shows the way in which the heating time affects the weld displacement curves for resistance welding of GF/PEI laminates with 0.1 wt% residual moisture under a power input of 80 kW/m^2, 0.8 MPa welding pressure and 100, 50 and 30 s heating times. The three following main effects could be observed:

- As expected, decreasing the heating time led to a decreased number of stages in the weld displacement curves since some physical phenomena do not get to occur during the welding process when the time is not long enough. As an example, for 55 s heating time no stage iii could be found in the displacement curve, indicating absence of squeeze flow. Likewise, for the joints welded with an even shorter heating time, i.e. 30 s, only three stages could be clearly identified in the displacement curve, namely stages i, iv and v.
- The peak displacement at the end of stage ii was lower for decreased heating time. This results from the fact that shorter heating times lead to lower welding

temperatures and there is hence less thickness increase resulting from thermal expansion and void formation.

- The displacement at stage v increased for increasing heating times. For 30 s heating time, the final thickness of the measured stack coincided with its initial thickness. However, for 55 s and 100 s heating times final thicknesses were higher than the initial one. Even though squeeze flow occurred in the case of 100 s heating time, the final to initial thickness gap was higher for 100 than for 55 s heating time. This phenomenon was associated to the occurrence of increased porosity with increased welding temperature, i.e. increased heating time, as seen in the micrographs in Fig 7. In the case of 30 s welding time, the welding temperature was too low to promote void formation and therefore no thickness increase occurred as a result of the welding process.

3.3. Effect of welding pressure on the weld displacement curve

The effect of welding pressure on the displacement curve was studied for resistance welding of GF/PEI laminates with 0.1 wt% residual moisture under a power input of 80 kW/m^2 and a 100 s heating time. The displacement curves corresponding to welding pressures of 0.2 MPa, 0.8 MPa and 1.5 MPa are shown in Fig.8. The major observations are the following:

- Decreasing the welding pressure led to higher rates at which displacement increases during stage ii of the process. It also yielded higher peak and higher final displacement values. All these phenomena were attributed to increased void formation with decreased welding pressure, as known from literature [27, 28] and confirmed by the cross-section micrographs shown in Fig. 10. It should be noted that at the highest welding pressure of 1.5 MPa, for which significantly

less porosity was found on the cross-section micrographs, the final thickness of the stack was somewhat lower than the initial one. This was attributed to the occurrence of squeeze flow during the welding process as indicated by the displacement curve (Fig. 8) and the micrographic inspection of the welded joints (Fig. 9)

- The weld displacement curve for the lowest welding pressure of 0.2 MPa showed no stage iii, which is in accordance with the observation of no significant resin flash in the welded joints (Fig. 10). This results from the low welding pressure not being able to induce squeeze flow in the highly viscous PEI resin.

3.4. Effect of residual moisture on the weld displacement curve

Even though the weld displacement curves obtained using adherends with 0.1 wt% residual moisture showed distinctive stages that could be related to the physical changes expected during the welding process, experiments on adherends with different moisture content were carried out in this section for further understanding of the effect of residual moisture on the weld displacement curves. Fig. 10 shows the welding displacement curve for fully dried adherends (dried in an oven at 135°C for 8 hours) at 80 kW/m^2 input power, 130 s heating time and 0.8 MPa welding pressure. Fig. 11 shows weld displacement curves for fully dried adherends and adherends with 0.1 and 0.3 wt% residual moisture at 80 kW/m^2 input power, 55 s heating time and 0.8 MPa welding pressure. Finally, Fig. 12 shows representative cross-sectional micrographs of the welds which displacement curves are shown in Fig. 11. The main observations drawn from these results are the following:

- Variations in the moisture content in the adherends did not cause changes in the shape of the weld displacement curves and the stages they define, as it can be seen for adherends with 0.1 wt.% moisture content and dry adherends in Figs. 3 and 10, respectively.
- Increased moisture content in the adherends resulted in increased porosity in the welding stack (Fig. 12). Void formation during the welding process had, as expected, a significant effect in the displacement rate within stage ii. Higher displacement rates, believed to be caused by higher void formation and growth rates upon heating, were obtained for higher moisture contents (Fig. 11). Peak displacement values were consequently higher for higher moisture content. It must be noted that, since the heating time used in the experiments which results are shown in Fig. 12 was only 55 s, no squeeze flow, and thus stage iii, was observed and peak displacement values were obtained when the power supply was switched off.
- Due to increased porosity in the adherends with increased moisture content, the final displacement values, i.e. displacement in stage v, were higher for higher moisture content. It must be noted though that the final displacement values for welded joints with fully dry adherends were slightly positive, indicating a slight thickness increase in the welding stack during the welding process. This thickness increase could be caused by a certain de-compaction or local relaxation of the residual compressive stresses in the fabric reinforcement [28], since the welding pressure, 0.8 MPa, was significantly lower than the consolidation pressure used for the manufacturing of the composite laminates, 2

MPa. This de-compaction was however not enough to cause any observable voids or resin rupture in the adherends (Fig. 12).

3.5. Definition of processing window based on weld displacement data

As discussed above, the physical phenomena that take place during the welding process, such as intimate contact, thermal expansion/contraction and resin squeeze flow, can be identified in the weld displacement curves. Therefore, they can be used for the definition of processing windows by determining appropriate time ranges for different input power levels. The proposed procedure would be as follows:

i. Obtaining of a complete weld displacement curve, i.e. with a long enough heating time to display all the five stages defined in 3.2 for the considered power level.

ii. Definition of a lower boundary for the heating time in the displacement curve. Due to the relatively short time required for molecular inter-diffusion once intimate contact is achieved in the welding process [14,29,30], the end point of stage i is proposed as the lower boundary for the heating time.

iii. Definition of an upper boundary for the heating time in the displacement curve. Since resin squeeze flow has been shown to negatively affect dimensional stability and mechanical performance of welded joints [6-8], the onset of stage iii is proposed as the upper boundary for the heating time.

In order to validate this approach, welding time ranges defined through displacement data (denoted as displacement-based processing window) were compared to welding time ranges defined through weld lap shear strength testing (denoted as LSS-based processing window) for the different sets of welding conditions listed in Table 1. Based

on the procedure most commonly used in literature, a threshold LSS, calculated as 80% of the maximum average LSS obtained in the tests, was used to define the lower and upper limit of the LSS-based processing windows [9]. Since, for all the conditions listed in Table 1, the maximum average LSS was found to be 32.1 MPa, the LSS threshold was set at 25.6 MPa. It must be noted that only one welded panel per set of welding conditions was necessary for the definition of the displacement-based processing window, whereas multiple welded panels per set of welding conditions were necessary for the definition of the LSS-based processing window. The results of the comparison between displacement-based and LSS-based processing windows are shown in Figs. 13 to 15. The main observations drawn from these results are the following:

- In general, good agreement was found between displacement-based and LSS-based processing windows for either dry or wet adherends. In the case of 50 kW/m^2 power input, however, a LSS value considerably lower than the threshold was found for a heating time close to the lower edge but still within the displacement-based processing window. This can be explained by the fact that, when the power input is significantly low, welding times are considerably longer and hence there is more time for heat to be transferred away from the welding interface. As a result, temperate within the adherends and the insulation blocks is higher than for higher power input (see Fig. 16). Consequently, thermal expansion of adherends and insulation blocks has a bigger contribution to the displacement curves, which hence lose accuracy in describing the physical transformations occurring in the close neighbourhood of the welding interface.
- For all cases studied, the LSS reached its peak value approximately towards the middle of the displacement-based processing window. This could be used as a

rule for a fast approximate definition of the optimum heating time based on displacement data.

- A narrower processing window with shorter heating times was obtained for the joints welded using a higher power input, which results from the much faster heating of the welding interface.
- For a certain power level, the presence of moisture in the adherends was found to shift the processing window towards shorter welding times. This is believed to result from an increase in the thermal insulation properties of the adherends due to the presence of voids and, therefore, a faster heating of the welding interface.

4. Conclusion

Weld displacement curves were obtained by measuring combined vertical displacement of the welding stack (i.e. heating element and adherends) and the adjacent insulation blocks during resistance welding of glass fibre reinforced polyetherimide with a stainless steel mesh heating element. Relationships between the different events in the weld displacement curves and the physical phenomena taking place during the welding process were investigated. As a result, a displacement-based approach for the definition of processing windows was proposed and validated. The main conclusions of this investigation are:

- Despite the fact that the thickness variations in the welding stack could not be directly measured, the weld displacement curves obtained in this research showed five distinct stages that could be related to physical phenomena taking

place at the welding interface and the adherends during the welding process. In particular, physical changes very localised at the welding interface, such as intimate contact or squeeze flow could be detected in the weld displacement curves.

.

- Formation of voids during the welding process did not affect the general shape of the weld displacement curves and the stages they defined. Nevertheless, void formation was found to affect the rate at which displacement increases upon heating as well as the final thickness of the welding stack. This indicates that early detection of process-induced porosity should be possible through displacement monitoring during the welding process.
- Processing windows based on displacement data with heating times delimited by the occurrence of intimate contact and of squeeze flow at the welding interface showed good agreement with traditional processing windows based on mechanical testing. The experimental work load associated to the definition of displacement-based processing windows was however substantially lower. Therefore, the method proposed in this paper for the definition of processing windows based on displacement data is considered of significant importance for the reduction of the lead time associated to the development of resistance-welded thermoplastic composite structures.

Acknowledgements

The authors would like to express their gratitude for the support provided by TenCate Advanced Composites, The Netherlands. H. Shi thanks the PhD Scholarship Fund from China Scholarship Council (CSC) for overseas study.

References

1. Ageorges C, Ye L. Fusion Bonding of Polymer Composites. London: Springer-Verlag; 2002.
2. Yousefpour A, Hojjati M, Immarigeon J-P. Fusion Bonding/Welding of Thermoplastic Composites. Journal of Thermoplastic Composite Materials. 2004;17(4):303-41.
3. Stavrov D, Bersee HEN. Resistance welding of thermoplastic composites-an overview. Composites Part A: Applied Science and Manufacturing. 2005;36(1):39-54.
4. Ageorges C, Ye L, Hou M. Experimental investigation of the resistance welding for thermoplastic-matrix composites. Part I: heating element and heat transfer. Composites Science and Technology. 2000;60(7):1027-39.
5. Hou M, Yang M, Beehag A, Mai Y, Ye L. Resistance welding of carbon fibre reinforced thermoplastic composite using alternative heating element. Composite Structures. 1999;47(1-4):667-72.
6. Hou M, Ye L, Mai YW. An Experimental Study of Resistance Welding of Carbon Fibre Fabric Reinforced Polyetherimide (CF Fabric/PEI) Composite Material. Applied Composite Materials. 1999;6(1):35-49.
7. Ageorges C, Ye L, Hou M. Experimental investigation of the resistance welding of thermoplastic-matrix composites. Part II: optimum processing window and

mechanical performance. Composites Science and Technology. 2000;60(8):1191-202.

8. Stavrov D, Bersee HEN. Experimental investigation of resistance welding of thermoplastic composites with metal mesh heating element. SAMPE-Europe conference proceedings. Paris, France2004.
9. Stavrov D, Bersee HEN, Beukers A. Resistance Welding of Continuous Fibre Reinforced PPS Composites with Metal Mesh Heating Element. 1st International Conference on Innovation and Integration in Aerospace Sciences. Queen's University Belfast, Northern Ireland, UK.2005.
10. Shi H, Villegas IF, Bersee HEN. Strength and failure modes in resistance welded thermoplastic composite joints: Effect of fibre–matrix adhesion and fibre orientation. Composites Part A: Applied Science and Manufacturing. 2013;55(0):1-10.
11. Jakobsen TB, Don RC, Gillespie JW. Two-Dimensional thermal analysis of resistance welded thermoplastic composites. Polymer Engineering & Science. 1989;29(23):1722-9.
12. Maffezzoli AM, Kenny JM, Nicolais L. Welding of PEEK/carbon fiber composite laminates. SAMPE Journal. 1989;25(1):35-40.
13. Xiao XR, Hoa SV, Street KN. Processing and Modelling of Resistance Welding of APC-2 Composite. Journal of Composite Materials. 1992;26(7):1031-49.
14. Ageorges C, Ye L, Mai Y-W, Hou M. Characteristics of resistance welding of lap shear coupons. Part II. Consolidation. Composites Part A: Applied Science and Manufacturing. 1998;29(8):911-9.

15. Ageorges C, Ye L, Mai Y-W, Hou M. Characteristics of resistance welding of lap shear coupons. Part I. Heat transfer. Composites Part A: Applied Science and Manufacturing. 1998;29(8):899-909.
16. Shi H, Villegas IF, Bersee HEN. Modelling of Heat Transfer and Consolidation For Thermoplastic Composites Resistance Welding. 18th International Conference on Composites Materials. Jeju, South Korea2011.
17. Colak ZS, Sonmez FO, Kalenderoglu V. Process Modeling and Optimization of Resistance Welding for Thermoplastic Composites. Journal of Composite Materials. 2002;36(6):721-44.
18. Villegas IF, Bersee HEN. Characterisation of a metal mesh heating element for closed-loop resistance welding of thermoplastic composites. Journal of Thermoplastic Composite Materials. 2013.
19. Howie I, Gillespie JW, Smiley AJ. Resistance Welding of Graphite-Polyarylsulfone/Polysulfone Dual-Polymer Composites. Journal of Thermoplastic Composite Materials. 1993;6(3):205-25.
20. Duhamel JMC. Second memoire sur les phenomenes thermo-mecaniques. Journal de I'Ecole Poly technique. 1837;15(25):1-57.
21. Stavrov D, Bersee HEN, Beukers A. The Influence of the heating element on resistance welding of thermoplastic composite materials. ICCM-14 Conference. 2003.
22. Dubé M, Hubert P, Gallet JN, Stavrov D, Bersee HE, Yousefpour A. Metal mesh heating element size effect in resistance welding of thermoplastic composites. Journal of Composite Materials. 2012;46(8):911-9.

23. Shi H, Villegas IF, Bersee HEN. An investigation on the strain distribution of resistance welded thermoplastic composite joints. 53rd AIAA/ASME/ASCE/AHS/ASC Structures, Structural Dynamics, and Materials Conference. Honolulu, Hawaii.: AIAA; 2012.
24. Roychowdhury S, Jr. JWG, Advani SG. Volatile-induced Void formation in amorphous thermoplastic polymeric materials : I. Modeling and parametric studies. London, ROYAUME-UNI: Sage; 2001.
25. Arefmanesh A, Advani SG, Michaelides EE. An accurate numerical solution for mass diffusion-induced bubble growth in viscous liquids containing limited dissolved gas. International Journal of Heat and Mass Transfer. 1992;35(7):1711-22.
26. Vegt AKvd. From Polymers to Plastics. Delft: Delft Academic Press; 2006.
27. Ye L, Lu M, Mai Y-W. Thermal de-consolidation of thermoplastic matrix composites--I. Growth of voids. Composites Science and Technology. 2002;62(16):2121-30.
28. Henninger F, Ye L, Friedrich K. Deconsolidation behaviour of glass fibre-polyamide 12 composite sheet material during post-processing. Plastics Rubber and Composites Processing and Applications. 1998;27(6):287-92.
29. Butler CA, Mccullough RL, Pitchumani R, Gillespie JW. An Analysis of Mechanisms Governing Fusion Bonding of Thermoplastic Composites. Journal of Thermoplastic Composite Materials. 1998;11(4):338-63.
30. Benatar A, Gutowski TG. Ultrasonic welding of PEEK graphite APC-2 composites. Polymer Engineering & Science. 1989;29(23):1705-21.

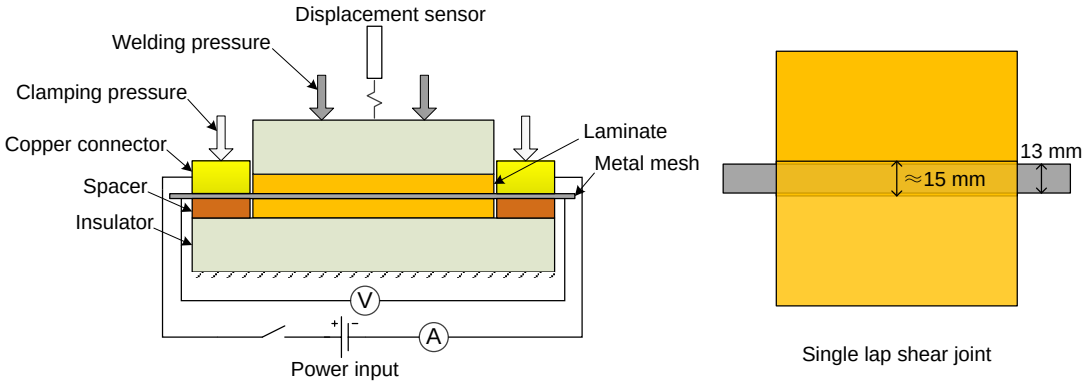

Fig.1. Schematic of resistance welding setup with displacement sensor.

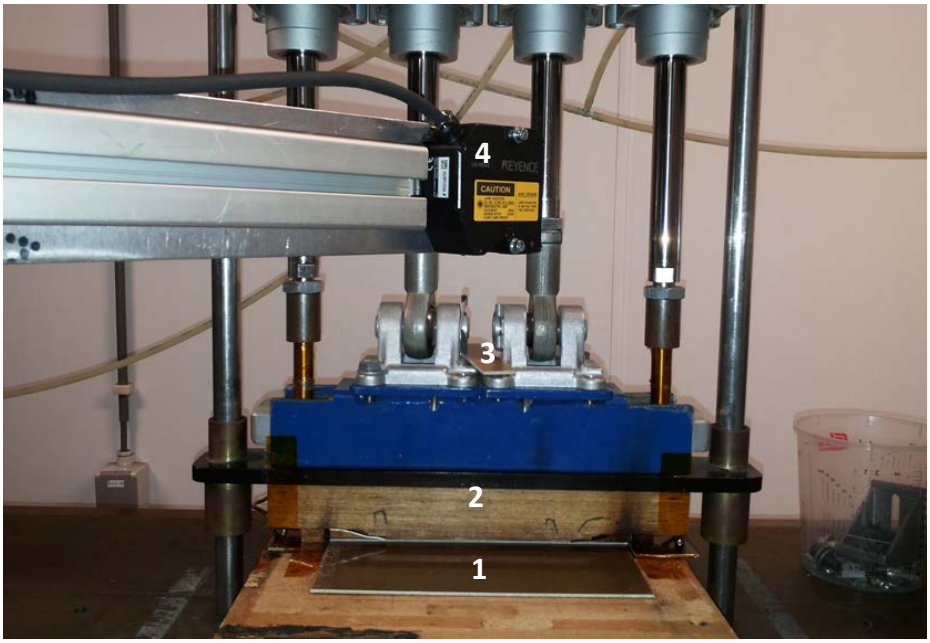

Fig.2. Displacement measurement during resistance welding: 1) welding stack, 2) thermal insulation block, 3) reference plane on holder of thermal insulation block for displacement measurement, and 4) laser displacement sensor.

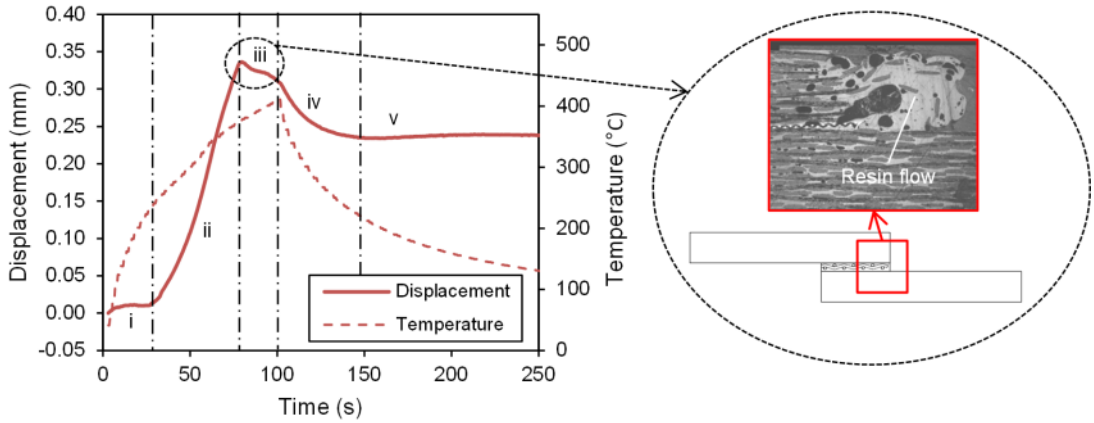

Fig.3. Temperature and weld displacement curves for resistance welding of GF/PEI laminates (0.1 wt% residual moisture, 80 kW/m^2 power input, 0.8 MPa welding pressure, 100 s heating time). The weld displacement curve can be divided into five stages (i to v in the graph).

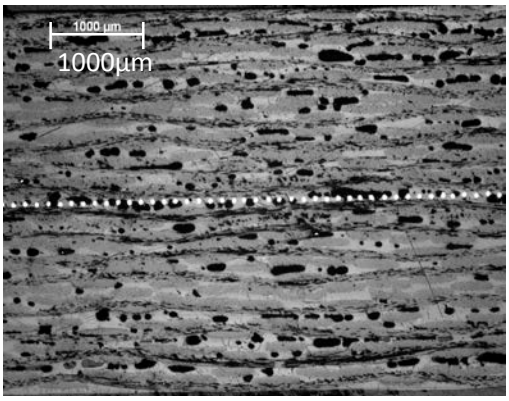

Fig. 4. Cross-section micrograph of GF/PEI welded sample showing significant porosity (0.1 wt% residual moisture, 80 kW/m^2 power input, 0.8 MPa welding pressure, 100 s heating time).

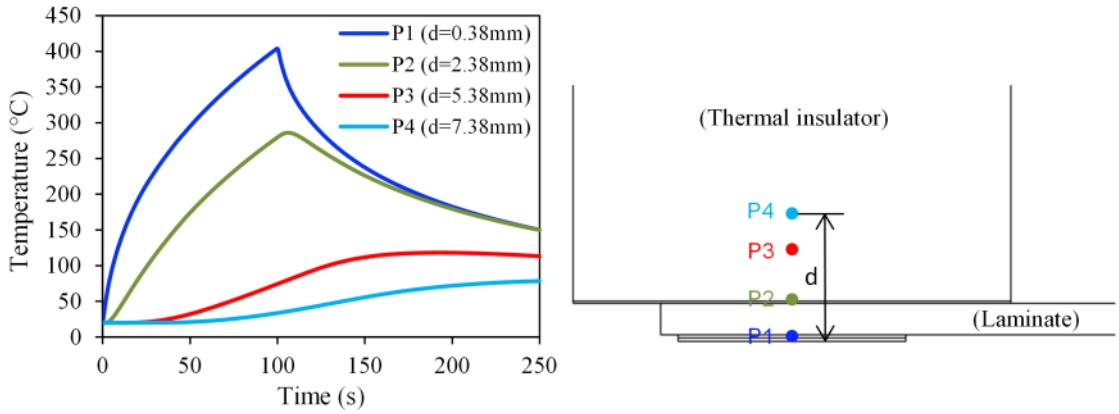

Fig.5. Temperature evolution at different locations away from the welding interface as predicted by the heat transfer model described in [16] (80 kW/m^2 input power).

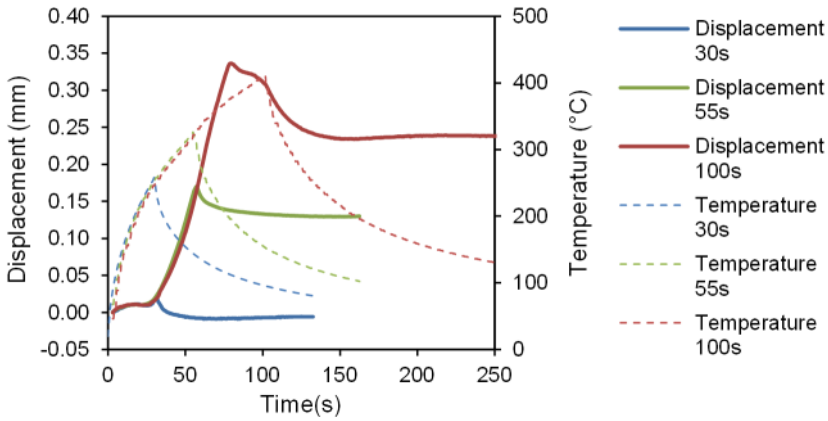

Fig.6. Temperature and weld displacement curves for resistance welding of GF/PEI laminates (0.1 wt% residual moisture, 80 kW/m^2 power input, 0.8 MPa welding pressure) under different heating times, 30 s, 55 s, and 100 s.

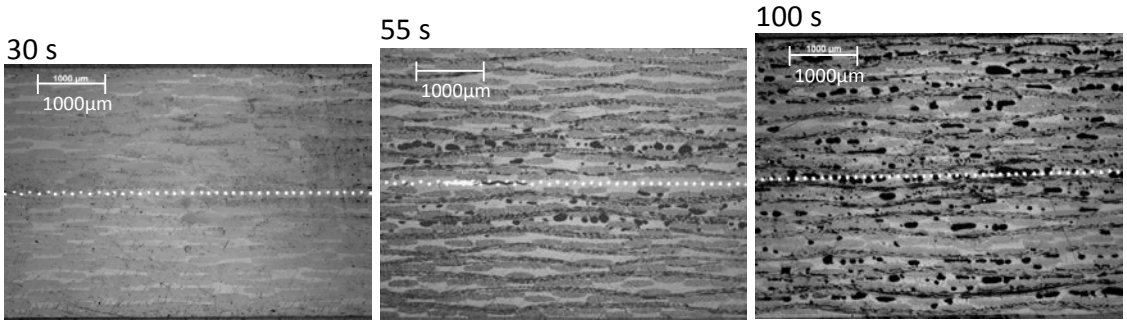

Fig. 7. Cross-section micrographs of GF/PEI welds (0.1 wt% residual moisture, 80 kW/m^2 power input, 0.8 MPa welding pressure) under different heating times, 30 s, 55 s, and 100 s.

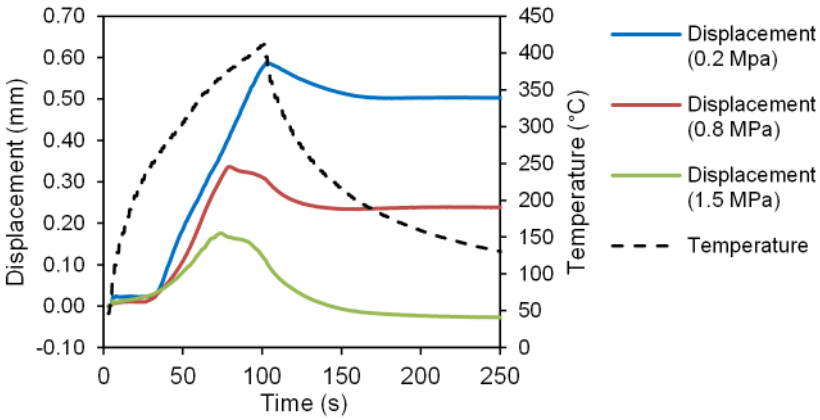

Fig.8. Weld displacement curves for resistance welding of GF/PEI laminates (0.1 wt% residual moisture, 80 kW/m^2 power input, 100 s welding time) under different welding pressures, 0.2 MPa, 0.8 MPa and 1.5 MPa. Temperature evolution for 0.8 MPa welding pressure.

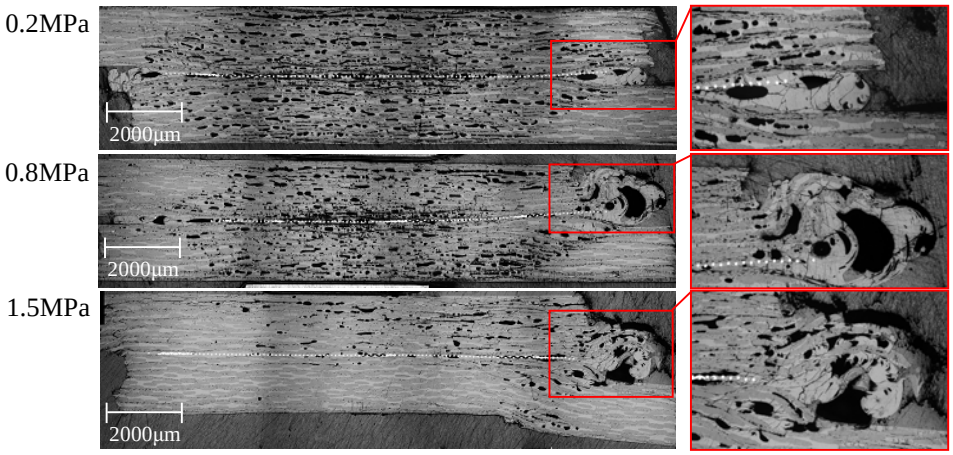

Fig.9. Cross-section micrographs of resistance welded GF/PEI laminates (0.1 wt% residual moisture, 80 kW/m^2 power input, 100 s welding time) under different welding pressures, 0.2 MPa, 0.8 MPa and 1.5 MPa.

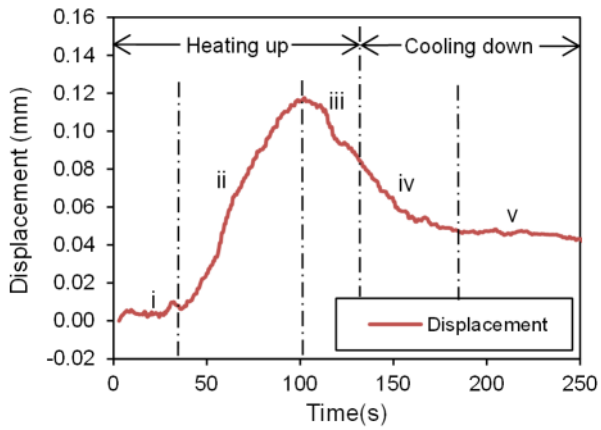

Fig.10. W displacement curve for resistance welding of fully-dried GF/PEI laminates (80 kW/m^2 power input, 0.8 MPa welding pressure, 130 s heating time).

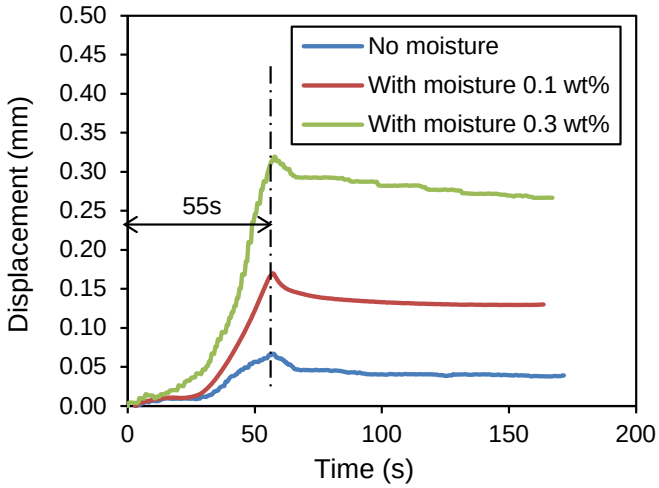

Fig.11. Weld displacement curves for resistance welding of GF/PEI laminates (80 kW/m^2, 0.8 MPa welding pressure and 55 s heating time) with 0 wt%, 0.1 wt%, and 0.3 wt% residual moisture.

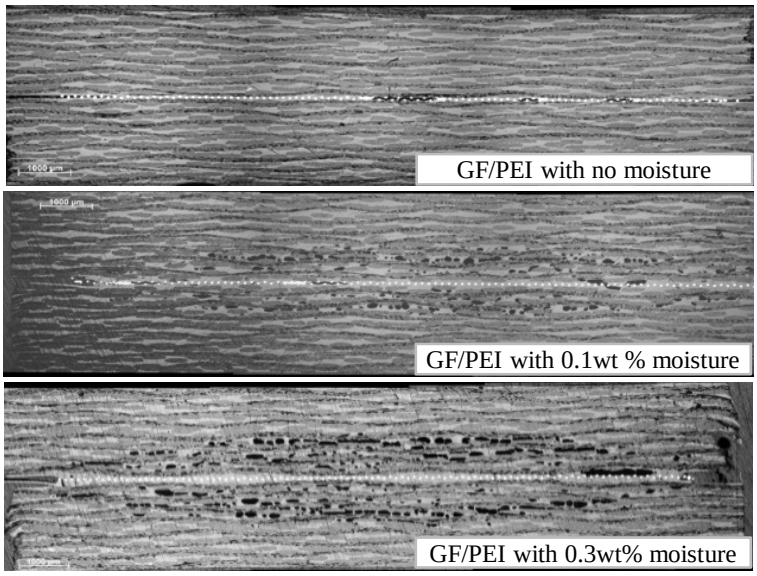

Fig.12. Cross-section micrographs of resistance welded GF/PEI laminates (80 kW/m^2, 0.8 MPa welding pressure and 55 s heating time) with 0 wt%, 0.1 wt%, and 0.3 wt% residual moisture.

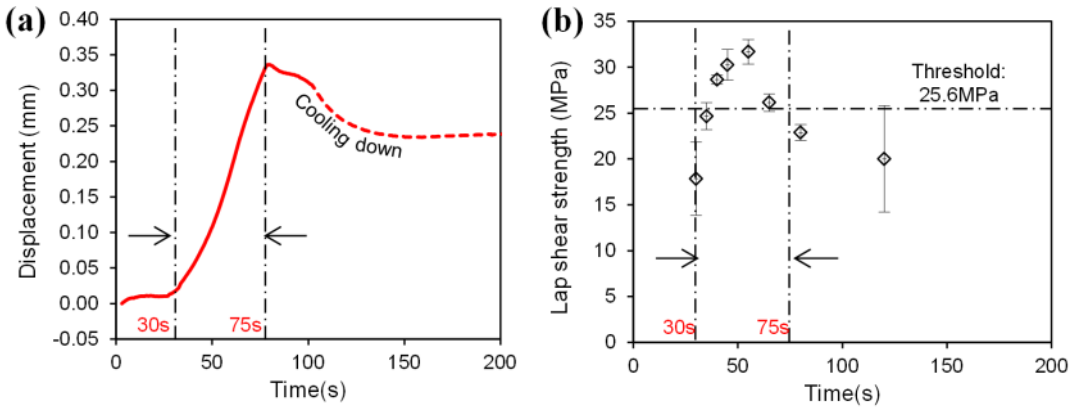

Fig.13. (a) Processing window defined using displacement data (b) processing window defined from mechanical tests (GF/PEI laminates with 0.1 wt% residual moisture, 80 kW/m^2 power input, 0.8 MPa welding pressure)

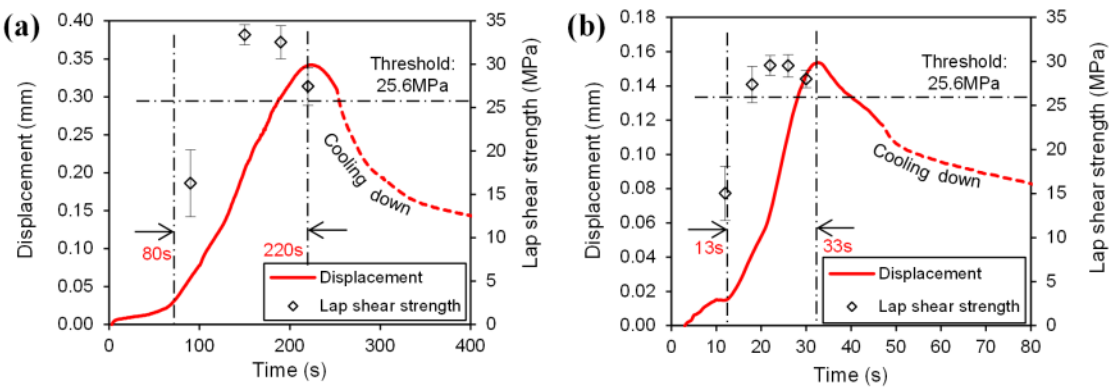

Fig.14. Displacement-based and LSS-based processing windows for (a) 50 kW/m^2 power input and (b) 120 kW/m^2 power input. (GF/PEI laminates with 0.1 wt% residual moisture, 0.8 MPa welding pressure).

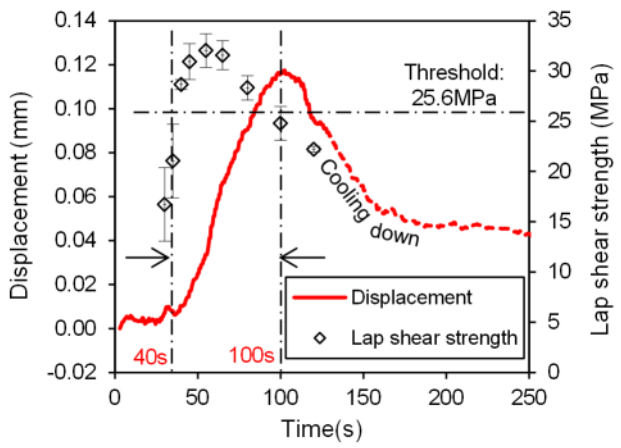

Fig.15. Displacement-based and LSS-based processing windows for fully dried GF/PEI laminates (80 kW/m^2 input power, 0.8 MPa welding pressure)

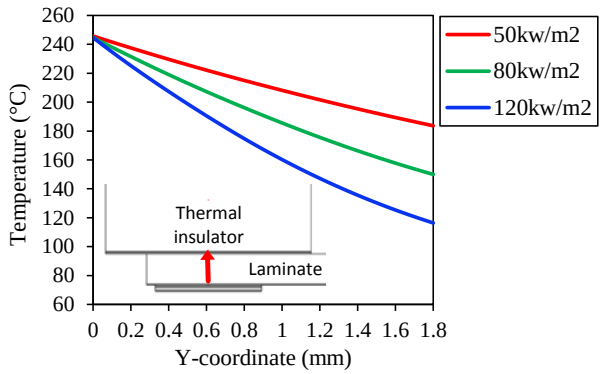

Fig. 16. Temperature distribution through the thickness for 50, 80 and 120 kW/m^2 input power as predicted by the heat transfer model described in [16].

Table 1. Different welding conditions for the validation of displacement-based processing window versus LSS-based processing window.

Power level (kW/m^2)	Welding pressure (MPa)	Moisture content in the GF/PEI adherends (% wt.)
80	0.8	0.1
50	0.8	0.1
120	0.8	0.1
80	0.8	0